Supplement of Atmos. Chem. Phys., 26, 10355–10377, 2026
https://doi.org/10.5194/acp-26-10355-2026-supplement

Supplement of

Sources and variability of surface ozone over the Tibetan Plateau revealed by in situ observations and EMAC model simulations

Yihan Zou et al.

Correspondence to: Jianzhong Ma (majz@cma.gov.cn) and Xiangdong Zheng (xdzheng@cma.gov.cn)

Table S1. List of major acronyms and their full names used in this study.

Acronym	Full Name
NHTS	Northern Hemisphere Mid-High Latitude Troposphere
TRTS	Tropical Troposphere
NTST	Northern Hemisphere and Tropical Stratosphere
NHTS-O_3	Ozone originating from NHTS
TRTS-O_3	Ozone originating from TRTS
NTST-O_3	Ozone originating from NTST
TP	Tibetan Plateau
NMC	Nam Co Comprehensive Observation Station
PYR	Nepal Climate Observatory at Pyramid

Table S2. Relative percentage contributions of 14 O_3 sources in the EMAC model to surface O_3 at NMC and PYR (3-year mean ± standard deviation) (units: %)

Source Name	NMC	PYR	Merged Source Name
Southern mid-high latitude troposphere (SHTS)	0.1±0.1	0.1±0.1	
Southern mid-latitude lower stratosphere (SMLS)	0.2±0.2	0.1±0.1	
Southern polar lower stratosphere (SPLS)	0.0±0.0	0.0±0.0	SH
Southern mid-latitude upper stratosphere (SMUS)	0.0±0.0	0.0±0.0	
Southern polar upper stratosphere (SPUS)	0.0±0.0	0.0±0.0	
Northern mid-latitude lower stratosphere (NMLS)	5.9±3.8	4.5±3.2	
Northern mid-latitude upper stratosphere (NMUS)	0.6±0.8	0.4±0.6	
Northern polar lower stratosphere (NPLS)	1.2±1.5	0.9±1.2	
Northern polar upper stratosphere (NPUS)	0.2±0.3	0.2±0.2	NTST
Tropical lower stratosphere (TRLS)	1.2±1.0	0.9±0.8	
Tropical middle stratosphere (TRMS)	0.0±0.1	0.0±0.1	
Tropical upper stratosphere (TRUS)	0.0±0.0	0.0±0.0	
Northern mid-high latitude troposphere (NHTS)	24.3±12.0	17.8±10.0	NHTS
Tropical troposphere (TRTS)	66.3±14.9	75.0±13.1	TRTS

Note:

(1) The daily relative percentage contributions from the Southern Hemisphere sources (SHTS, SMLS, SMUS, SPLS, SPUS) to surface O_3 at both stations were all below 1%; consequently, these Southern Hemisphere sources (highlighted in red) were ignored in the subsequent analysis.

(2) As our study focuses on the overall contribution of stratospheric sources rather than the differences among stratospheric sources at different latitudes, we merged the seven stratospheric source regions (NMLS, NMUS, NPLS, NPUS, TRLS, TRMS, TRUS; highlighted in blue), each of which contributed less than 10% to the 3-year average percentage contributions at both stations individually, into a single source category, namely the Northern Hemisphere and Tropical Stratosphere (NTST).

(3) We retained the two tropospheric source regions, i.e., the northern mid-high latitude troposphere (NHTS) and the tropical troposphere (TRTS).

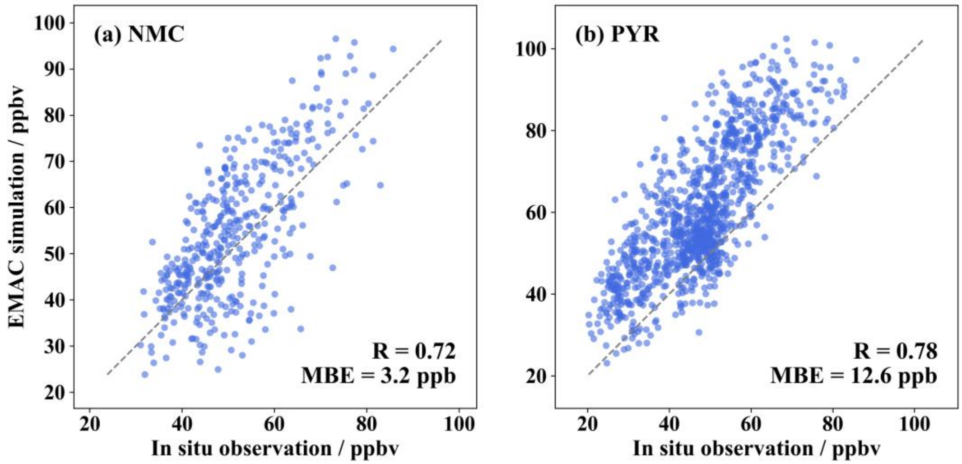

Figure S1. Scatter plot comparison of EMAC-simulated vs. observed daily surface ozone mixing ratios at NMC and PYR

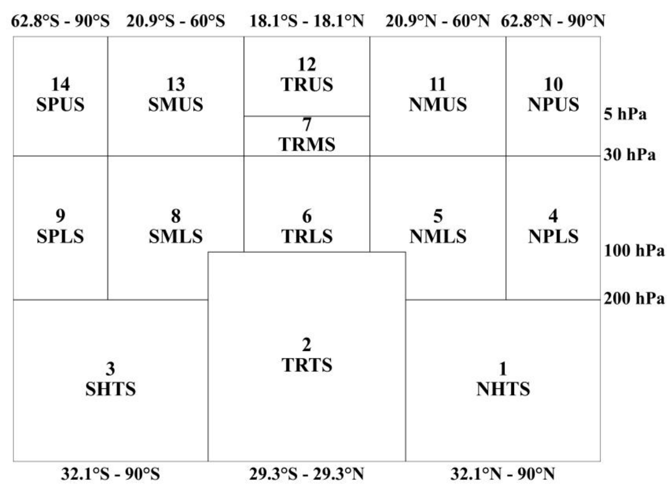

Figure S2. Division of O_3 source regions in the O3_ORIG submodule (adapted from Jöckel et al., 2016)

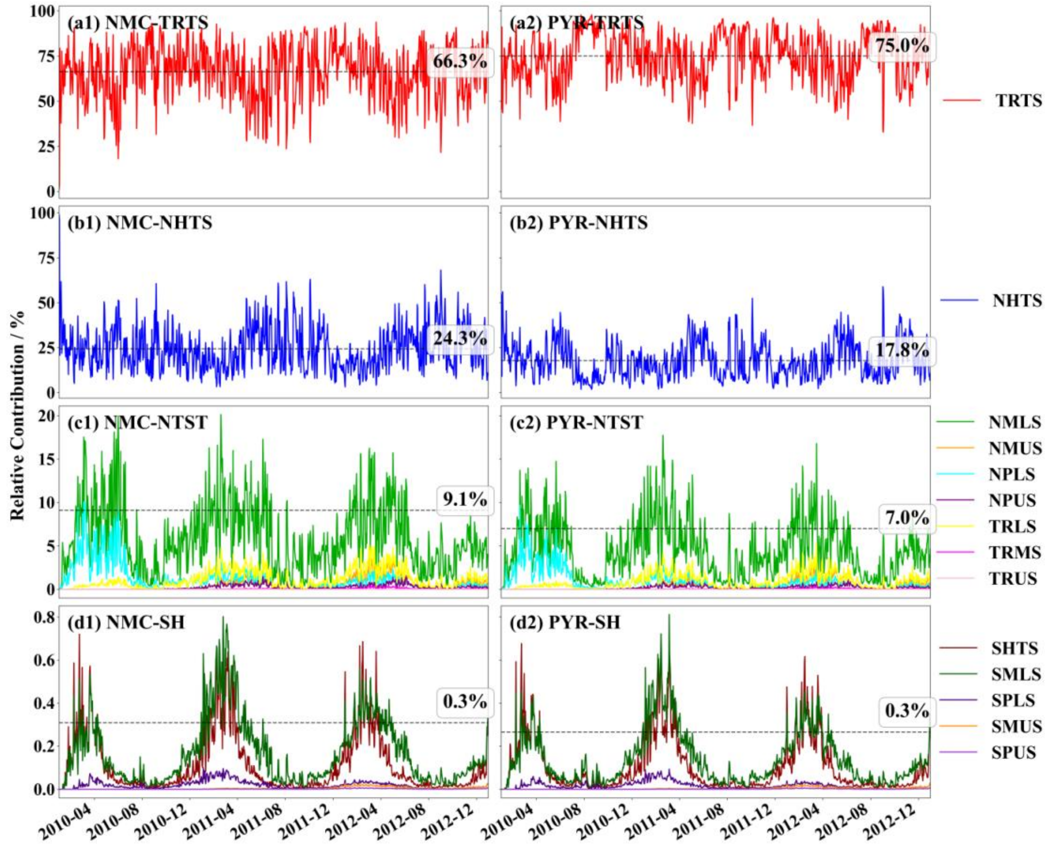

Figure S3. Line plots of the relative percentage contributions of 14 O_3 sources in the EMAC model to surface ozone at NMC (1) and PYR (2) during 2010–2012. Panels (a) to (d) correspond to the 4 merged ozone sources in sequence: TRTS (a), NHTS (b), NTST (c), and SH (d). Dashed lines denote the 3-year mean relative percentage contributions of the 4 merged ozone sources.

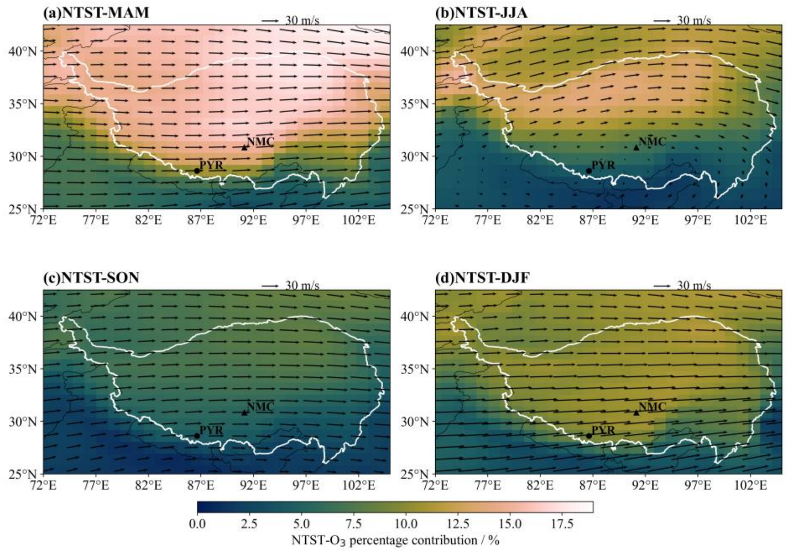

Figure S4. EMAC simulated regional distributions of surface NTST-O_3 relative contributions (fraction of tagged O_3 in total modelled O_3) and 200 hPa wind field over the Tibetan Plateau in different seasons during 2010-2012: (a) Spring, (b) Summer, (c) Autumn, (d) Winter. Color shading denotes NTST-O_3 relative contributions (units: %), and black arrows represent the wind field (units: m/s). White lines refer to the 3 km terrain height contour. Black dots mark the locations of the PYR (circle) and NMC (triangle) stations.

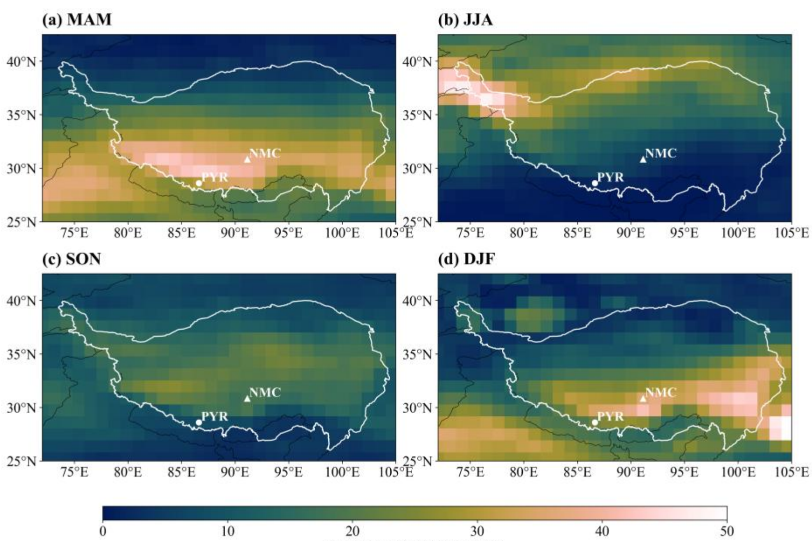

Figure S5. EMAC simulated regional distributions of seasonal mean tropopause fold frequency over the Tibetan Plateau during 2010-2012: (a) Spring, (b) Summer, (c) Autumn, (d) Winter. Color shading denotes the occurrence frequency of tropopause folds (units: %), calculated based on the 3D labeling algorithm. White lines refer to the 3 km terrain height contour, highlighting the Tibetan Plateau area. White dots mark the locations of the PYR (circle) and NMC (triangle) stations.

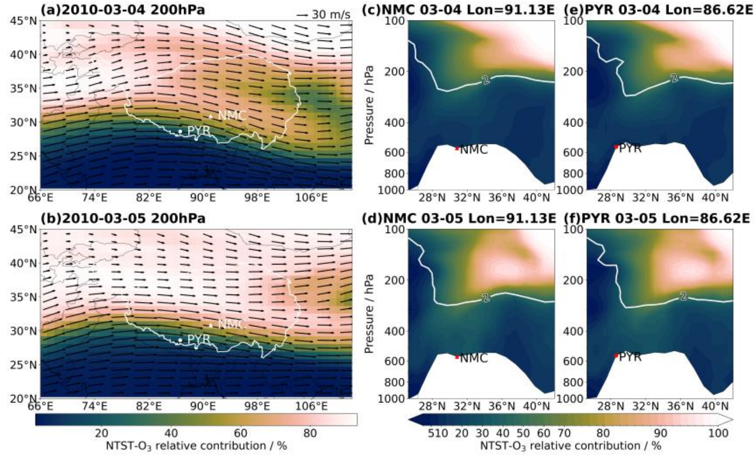

Figure S6. Upper-level tracer distribution and vertical dynamical structure of a stratospheric intrusion event in spring 2010 simulated by the EMAC model: Row 1 (a, c, e) corresponds to 4 March 2010, and Row 2 (b, d, f) corresponds to 5 March 2010. Column 1 (a, b) shows the regional distributions of NTST-O_3 relative contribution at 200 hPa (color shading) overlaid with wind fields (arrows); White lines highlight the Tibetan Plateau area, and white dots mark the locations of the PYR (circle) and NMC (triangle) stations. Column 2 (c, d) and Column 3 (e, f) present the meridional cross-sections of NMC (Lon=91.13°E) and PYR (Lon=86.62°E), respectively; thick white solid lines denote 2 PVU isopleths, red dots indicate the station locations, and color shading represents NTST-O_3 relative contribution (fraction of tagged O_3 in total modelled O_3, units: %)

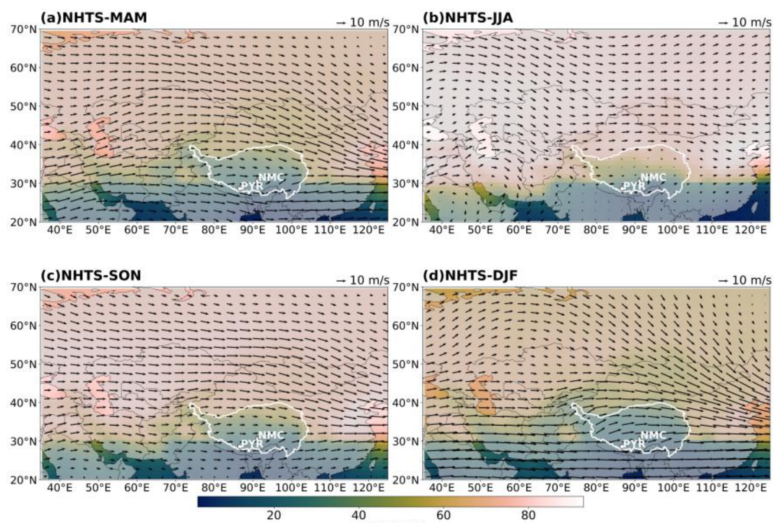

Figure S7. EMAC simulated regional distributions of surface NHTS-O_3 relative contribution (fraction of tagged O_3 in total modelled O_3) and 500 hPa wind field over parts of Eurasia (35°E-125°E, 20°N-70°N) in different seasons averaged over the period 2010-2012: (a) Spring, (b) Summer, (c) Autumn, (d) Winter. Color shading denotes NHTS-O_3 relative contribution (units: %), and black arrows represent the wind field (units: m/s). White lines highlight the Tibetan Plateau area, and white dots mark the locations of the PYR (circle) and NMC (triangle) stations.

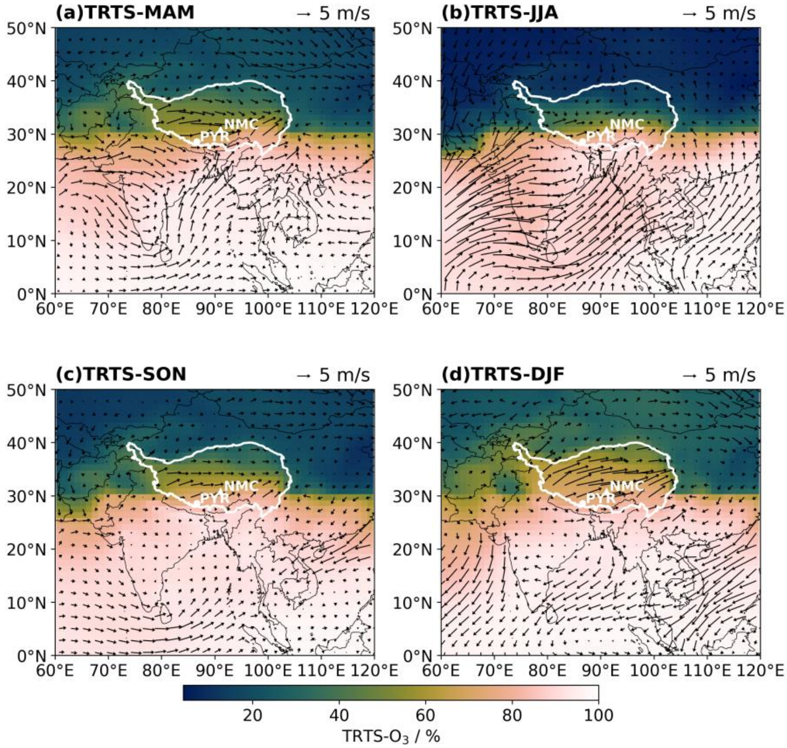

Figure S8. EMAC simulated regional distributions of surface TRTS-O_3 relative contribution (fraction of tagged O_3 in total modelled O_3) and boundary layer average wind field over a larger area covering the Tibetan Plateau, South Asia, and Southeast Asia in different seasons averaged over the period 2010–2012: (a) Spring, (b) Summer, (c) Autumn, (d) Winter. Color shading denotes TRTS-O_3 relative contribution (units: %), and black arrows represent the wind field (units: m/s). White lines highlight the Tibetan Plateau area, and white dots mark the locations of the PYR (circle) and NMC (triangle) stations.

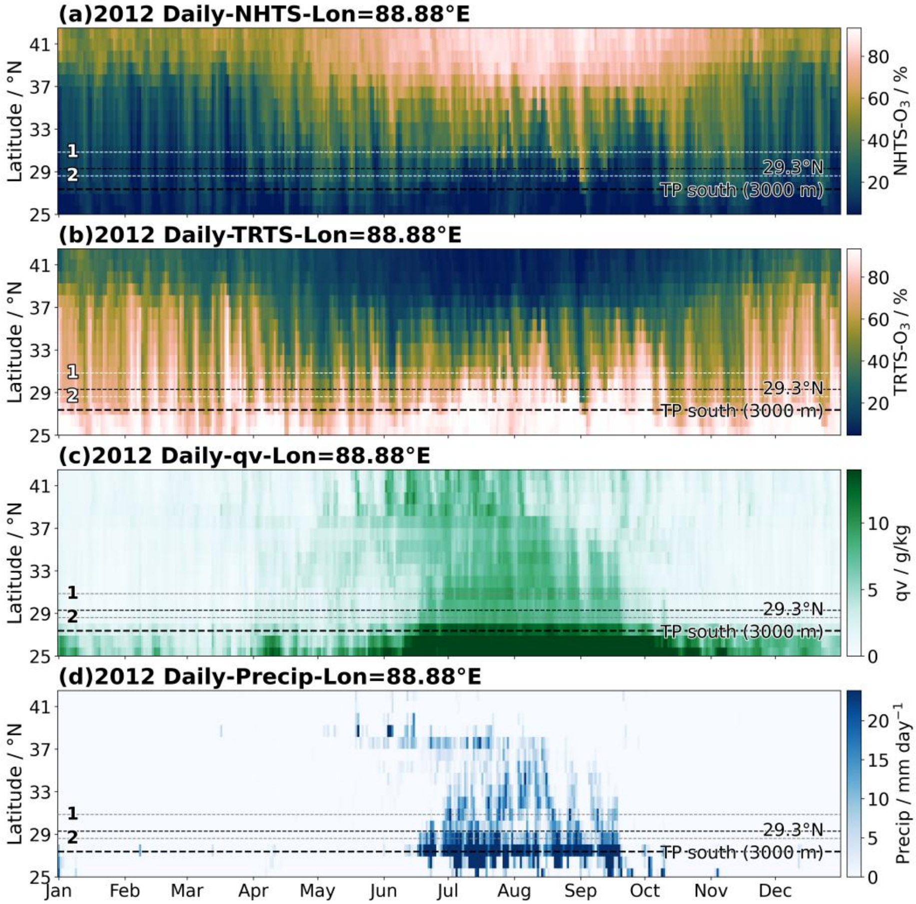

Figure S9. Time series of daily average surface (a) NHTS-O_3 relative contribution (fraction of NHTS-O_3 in total modelled O_3, units: %), (b) TRTS-O_3 relative contribution (fraction of TRTS-O_3 in total modelled O_3, units: %), (c) specific humidity (qv, units: g kg^{-1}), and (d) precipitation (units: mm day^{-1}) over the Tibetan Plateau at 88.88°E longitude (the midpoint of the longitudes of the two stations, NMC and PYR) in 2012, simulated by the EMAC model. The latitude 29.3°N (the boundary between the NHTS and TRTS source regions) is marked by a black dashed line, and dashed gray lines with numbered labels indicate the latitudes of the two stations (with "1" for NMC and "2" for PYR). The thick black dashed line indicates the southern boundary of the Tibetan Plateau at this longitude.

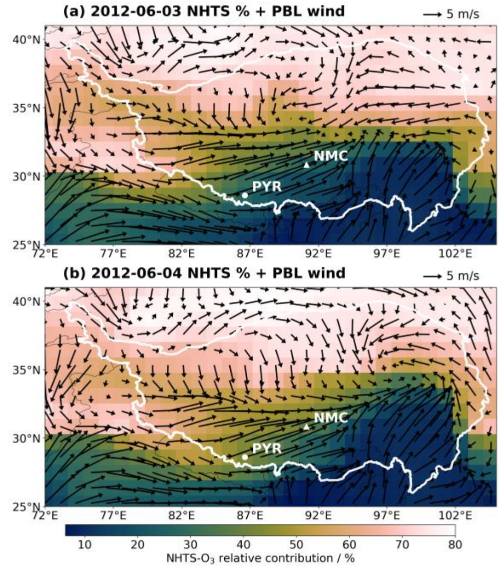

Figure S10. EMAC simulated changes in the regional distribution of surface NHTS-O_3 relative contribution (fraction of tagged O_3 in total modelled O_3, color shading, units: %) and the boundary layer average wind field (arrows, units: m/s) during a typical NHTS-O_3 transport event over the Tibetan Plateau: (a) corresponds to 3 June 2012, and (b) corresponds to 4 June 2012. White lines highlight the Tibetan Plateau area, and white dots mark the locations of the PYR (circle) and NMC (triangle) stations.

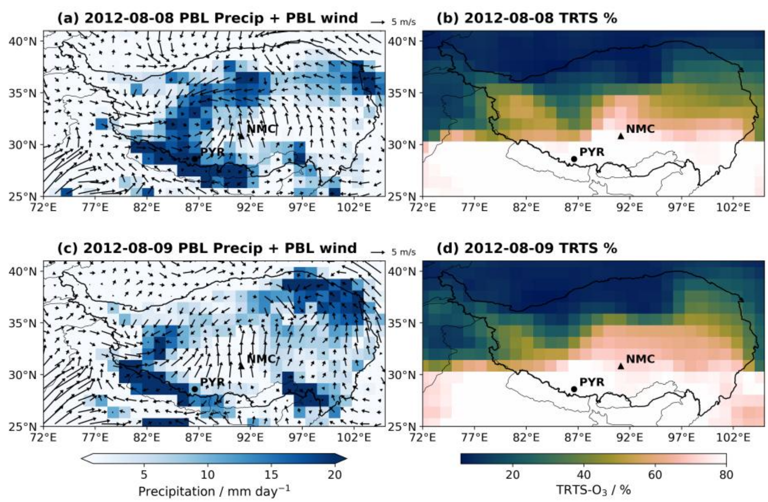

Figure S11. EMAC simulated changes in the regional distribution of surface TRTS-O_3 for a typical TRTS-O_3 transport event during the 2012 Asian summer monsoon: Row 1 (a, b) corresponds to 8 August 2012, and Row 2 (c, d) corresponds to 9 August 2012. Column 1 (a, c) shows the regional distributions of daily accumulated precipitation (color shading, units: mm day^{-1}) overlaid with the boundary layer average wind field (arrows, units: m/s). Column 2 (b, d) presents the regional distributions of surface TRTS-O_3 relative contribution (fraction of tagged O_3 in total modelled O_3, units: %). Black lines highlight the Tibetan Plateau area, and black dots mark the locations of the PYR (circle) and NMC (triangle) stations.

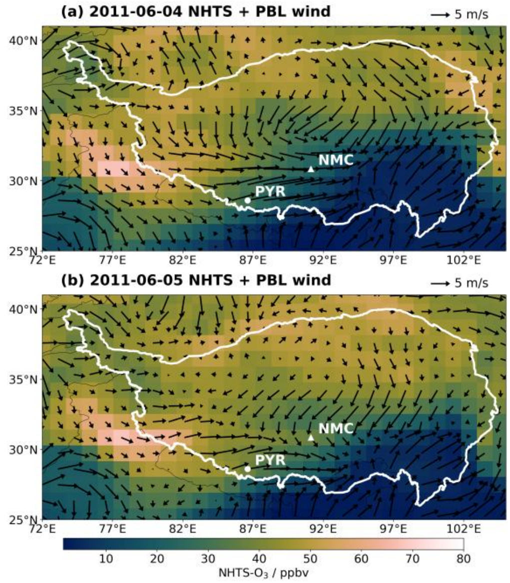

Figure S12. EMAC simulated changes in the regional distribution of surface NHTS-O_3 (color shading, units: ppbv) and the boundary layer average wind field (arrows, units: m/s) during a typical NHTS-O_3 transport event over the Tibetan Plateau: (a) corresponds to 4 June 2011, and (b) corresponds to 5 June 2011. White lines highlight the Tibetan Plateau area, and white dots mark the locations of the PYR (circle) and NMC (triangle) stations.

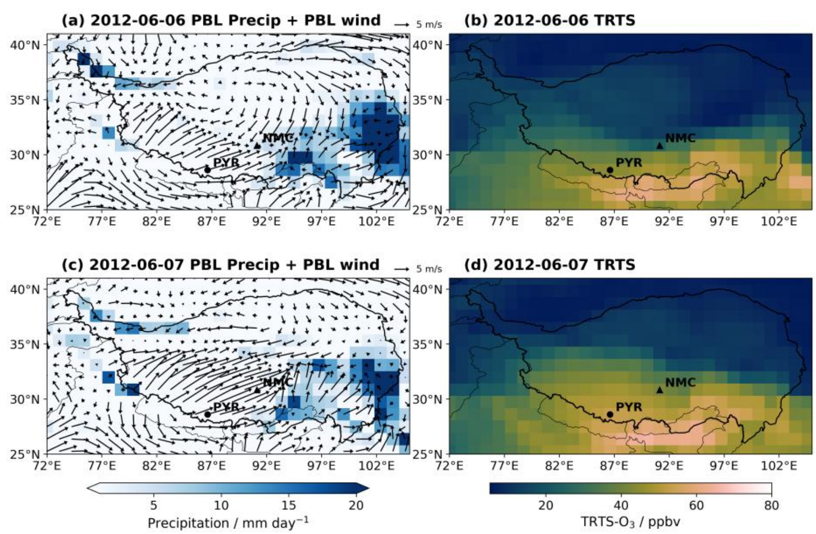

Figure S13. EMAC simulated changes in the regional distribution of surface TRTS-O_3 for a typical TRTS-O_3 transport event during the 2012 Asian summer monsoon: Row 1 (a, b) corresponds to 6 June 2012, and Row 2 (c, d) corresponds to 7 June 2012. Column 1 (a, c) shows the regional distributions of daily accumulated precipitation (color shading, units: mm day^{-1}) overlaid with the boundary layer average wind field (arrows, units: m/s). Column 2 (b, d) presents the regional distributions of surface TRTS-O_3 (units: ppbv). Black lines highlight the Tibetan Plateau area, and black dots mark the locations of the PYR (circle) and NMC (triangle) stations.